International Journal of Novel Researches in Science, Technology & Engineering
Vol. 5 No. 1 March, 2023
ISSN 2141 825X
www.oasisinternationaljournal.org

INFLUENCE OF SILVER NANO PARTICLES ON TIO_2 WITH ALPIRIN DYE: OPTICAL AND STRUCTURAL STUDY

by

[1]Dike, Ijeoma I., Akoma, Chigozie S[2] and Ozuomba, Jude O.[3]

[1,2]Abia State Polytechnic Aba, Abia State-Nigeria

[3]Imo State University Owerri, Imo State- Nigeria

Abstract

Sol-gel derived Titanium (iv) oxide (TiO_2) was deposited on to substrate glass using the screen printing technique. Silver nanoparticles (AgNPs) were deposited unto the TiO2 samples through the successive ionic layer adsorption and reaction method. The samples were soaked into the novel alpirin and were investigated. The films were characterized by Surface Profilometry, Ultraviolet –Visible light Spectroscopy (UV-Vis Spec) X-ray Diffraction (XRD) and Energy Dispersive Spectroscopy (EDS). The Surface Profilometry indicates that the samples were thin films. XRD results showed crystalline structure of titanium dioxide. Crystal phase observed for TiO_2 soaked in alpirin dye and the sample that served as control are anatatase structure. The average crystallite size of titanium dioxide when soaked into Alpirin was found to be 21.39 nm with average dislocation density of $2.597 \times 10^{-3} \text{lines/nm}^2$ and band gap of 2.52 eV. However, the film with the combination AgNPs + Alpirin, has the average crystallite size of 18.26 nm with average dislocation density of 3.093×10^{-3} lines/nm^2 and the band gap of 2.00 eV as against the pure TiO_2 with average crystalline size of 20.37 nm and average dislocation density of $3.086 \times 10^{-3} \text{lines/nm}^2$and band gap of 3.65 eV. Optical absorbance for pure TiO_2 was low but increased when soaked with Alpirin and AgNPs + Alpirin. The results showed that all the films have high transmittance within the visible and near infra-red region though there was slight decrease when soaked with Alpirin and AgNPs + Alpirin. Absorption coefficient, extinction coefficient and optical conductivity increased on soaking with Alpirin and increased further when soaked with AgNPs + Alpirin. The synergy between AgNPs + Alpirin show that the incorporation of metal nanoparticle is beneficial for enhanced photoactivity. The presence of silver and some other substances in the sample were confirmed through Energy Dispersive x-ray Spectrometry (EDS).

Keywords: Silver Nano, TiO_2 & Alpirin dye.

1. Introduction

Titanium dioxide films have attracted huge scientific and technological interest [1]. It's unique properties such as high transmittance, high refractive index, relatively high energy conversion

efficiency, electronics, excellent chemical stability, non-toxicity to the environment and relatively cheap nature makes it a better prospect for optical applications. It is the most promising electron acceptor because it transports electrons easily [2; 3; 4;5]. When light of appropriate intensity shines on titanium (iv) oxide surface, pairs of electrons and holes are generated inside its crystal lattice. Free electrons are usually produced in the conduction band and the holes at the valence band [6]. However, the major limitation associated with using TiO_2 as a photoanode is the high electron hole recombination as a result of its wide band gap energy; which causes a small fraction of the solar light from the ultraviolet region to be utilized [7;8]. To maximize the photoactivity of TiO_2, it is necessary to reduce the wide band gap energy [1]. Recently, scientific efforts have drifted towards shifting the optical sensitivity of the titanium oxide from UV to the visible region [9] with metals and non-metals such as nitrogen [10], silver [4], iron, gold [11], copper [12]. Other researchers have indicated that the use of natural ruthenium dye [12], cynodon dactylon [7], sepia melianin [1] among other dyes which are cheap, abundant, renewable and ecofriendly have significantly modified the photoactivity of titanium dioxide. However, solar cells fabricated with co-doped TiO_2 proved to be more efficient. Alwan *et al.,* doped TiO_2 samples with Fe, Cu and mix Fe-Cu (that is a mixture of Cu and Fe) and observed that mix Fe-Cu has more power conversion efficiency than samples doped with single metal. Deposition of Ag on doped TiO_2 showed enhanced photovoltaic properties due to the synergistic effect between Ag and doped TiO_2, the Ag-NPs has dual effect on the performance of TiO_2 including the enhancement of the absorption coefficient and optical absorption due to surface plasmon resonance [13;14]. Incorporating a very small amount of metal into natural dye has not been fully explored. This research area still remains very economical due to the cheap source of the natural dye and its natural abundance and renewability. However, the photoactivity activity of TiO_2 also strongly depends on the preparation methods and on the post-treatment conditions [15;16]. Different methods have been used to synthesize TiO_2. These include gel method [17;18] vapour deposition method [8], hydrolysis of inorganic salts [4;19] chemical spray pyrolysis, sol-gel technique, hydrothermal treatment, and arc discharge method [20;21]. Currently, sol–gel is one of the most successful techniques on how to prepare nanosized metallic oxides with high photocatalytic activity [4;22]. Screen printing deposition technique is one of the most reported methods of producing the nanostructured metal-oxide layer within DSSCs [23;24;25]. This deposition technique produces films in large quantity with the use of relatively cheap and simple designs with excellent scales of economy [23;25;26]. The aim of this research is to investigate the doping influence of Alpirin natural dye (a non-edible dye extract from alpinia purpurata commonly called red ginger flower) as well as Alpirin +AgNPs on the optical and structural properties of sol gel derived titanium dioxide. The results obtained from this research will provide useful information for researchers and manufacturers involved in DSSCs for high photoactiviy through the use of cost effective methods.

2. 0: Experimental

2.1 Materials

The sol-gel derived TiO_2 was purchased from Solaronix Renewable Energy. *Alpinia purpurata* flower samples were collected from a flower garden in a residential compound in Abia State. Silver nitrate ($AgNO_3$), tin (ii) chloride, methanol and soda lime substrate glass were purchased from Allan's Resources. All the other materials used in this research work were supplied by Sheda Science and Technology Complex (SHESTCO) Abuja.

2.2 : Deposition of TiO_2

The substrate glass was cleaned with deionized water and ultrasonicated in isopropanol for about 10 minutes. TiO_2 nanoparticles were gradually screen printed unto substrate glass and annealed at *500^oC* for 70 minutes. The films were allowed to cool down to room temperature. That was a necessary condition to remove thermal stresses and avoid cracking of the glass or peeling off the *TiO_2* film [27].

2.3 : Deposition of Silver Nanoparticles

The substrate glass was cleaned and made hydrophilic and then immersed in 0.1 M tin (ii) chloride ($SnCl_2$) for 20 minutes then rinsed with distilled water for 20 minutes and ass/TiO_2 was left without soaking into the alpirin..

2.6 : Characterization and measurement

The thicknesses of samples were measured using a Veeco Dektak 150 profilometer. 6.2.0.1588 UV/Vis/NIR spectrophotometer was used for the optical study. The scanning for each sample was done thrice in the wavelength interval of 0 nm to 1000 nm and the various averaged curves were taken in order to obtain the absorbance, transmittance, reflectance, refractive index and optical

immersed in 0.01 M silver nitrate ($AgNO_3$) and rinsed with dilute hydrochloric acid (HCl). This process gave the structure glass/TiO_2/AgNPs with one complete Successive ionic layer and adsorption reaction (SILAR) cycle. SILAR method is relatively simple, cheap, and time-saving and can be carried out at room temperature. It offers an easy control to the thickness of the film or nanoparticle.

2.4 : Preparation of Natural Dye

1g of the dry Alpinia purpurata flower sample was soaked in methanol and HCl mixed in the ratio of 99:1 to form acidified methanol. The solution was vibrated on a magnetic Stirrer Hotplate78-1for twenty (20) mins at uniform acidity (pH of 3). Dye extract at the pH of 3 displays broad absorption peak in the 480-560nm range resulting from π - π* transitions due to the mixed contributions of the yellow–orange betaxanthins (480 nm) and of the red–purple betacyanin (540 nm) [28;29]. The solution was filtered to get the dye.

2.5 : Soaking Process

The samples with structures; glass/TiO_2 and glass/TiO_2/AgNPs were soaked into Alpirin for 48 hours. As reference, another sample with structure of gl

conductivity. Applying the energy conservation law shown in (1)

$$A + T + R = 1 \qquad (1)$$

(where A is the absorbance, T is the transmittance, R is the reflectance), the reflectance values were obtained as shown in (2) [30].

$$1 - (A + T) = R \qquad (2)$$

The refractive index (η) determines the extent of permeability at which light rays can

travel through a medium. Refractive index values of the samples were obtained from equation (3) [4;31].

$$\eta = \frac{(1+\sqrt{R})}{(1-\sqrt{R})} \qquad (3)$$

Extinction coefficient (k) for the samples were calculated using equation (4) given by [32].

$$k = \frac{\alpha \lambda}{4\pi} \qquad (4)$$

Where α is the absorption coefficient, λ is the wavelength and π is equal to 3.142. The X-ray diffraction pattern was recorded on a Rigaku Ultima IV X-ray diffractometer and processed using JCPDS card numbers. Debeye Scherer Equation shown in (5) was used to determine the crystallite sizes (D).

$$D = \frac{k\lambda}{\beta \cos\theta} \qquad (5)$$

Where K is a constant (0.89) called the shape factor, $\boldsymbol{\lambda}$ is the wavelength (1.54Å). $\boldsymbol{\beta}$ is the Full Width Half Maximum (FWHM), $\theta = 2$ Theta

The optical band gap E_g was estimated from the Tauc relation shown in Figure 6:

$$(\alpha h\nu) = B(h\nu - E_g)^n \qquad (6)$$

Where, B is a constant, ν is the transition frequency, h is Planck's constant, hν is the photon energy, α is the absorption coefficient and the exponent n = 2 for direct transition and E_g is given in Equation 7.

$E_g = h\nu = hc/\lambda$ (7)

c is the velocity of light = 3 x 10^8 ms^{-1}, λ is the wavelength in meters (m). h = 6.62x10^{-34}Js, since 1J = 1.602 x 10^{-19} eV. Substituting for these variables into Equation 7 gives

$$h\nu = hc/\lambda = 1.241/\lambda(\mu m) \qquad (8)$$

The analysis of chemical composition was carried out by Energy Dispersive Spectrometry (EDS).

3.0: Results and Discussions

3.1: Optical Analysis

Figure 1 shows the UV-Vis absorption spectra of undoped and doped TiO_2 samples. The absorption edge was shifted to the visible region due to doping with *alpirin* with peak at 390 nm. However, a relatively broad and stronger enhancement was observed as a result of the AgNPs + *alpirin* film with peak at 420 nm. The optical absorption enhancement is attributed to the intensified near-field surface plasmon resonance (SPR) of metallic AgNPs, which interacted with the dye molecule thereby enhancing dye absorption. This result is in agreement with those obtained by [3;14;29]. Figure 2 shows high transmittance for the samples, although there was slight decrease for the doped samples. This shows that the film can be used as optical windows in solar cell. The result agrees with those obtained by [2].

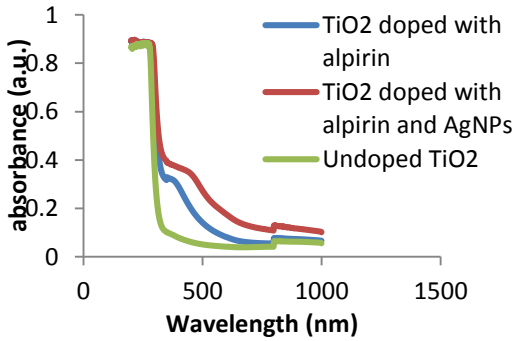

Fig. 1:Uv-vis spectra of undoped and doped TiO_2 samples

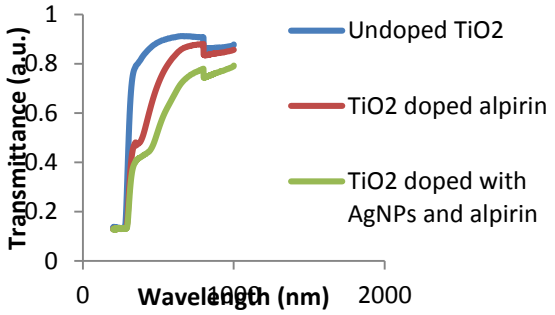

Fig. 2: Variation of transmittance with wavelength for undoped and doped TiO_2 samples

High reflectance in the visible region was observed in Figure 3 for the sample doped with *alpirin*, this increased further on doping with AgNPs + *alpirin*. This result is in agreement with [29].

The results obtained in Figure 4 indicate high refractive index within the visible region for sample doped with *alpirin* and further increase for doping with AgNPs + *alpirin*. This shows that the medium is highly permeable for light rays and very good for solar cell applications.

Figure 5 shows increased extinction coefficient for doping with *alpirin* and AgNPs + *alpirin* with peaks at 400 nm and 447 nm respectively due to increase in absorption.

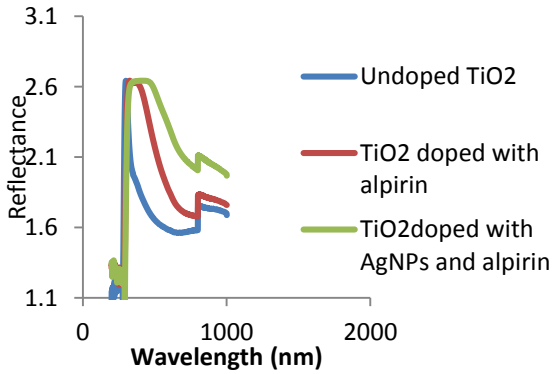

Fig. 3: Reflectance for undoped and doped TiO_2 samples

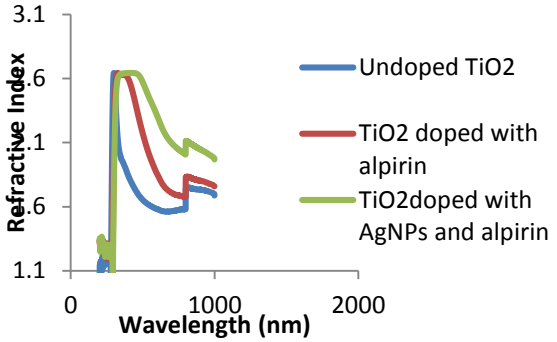

Fig. 4: Variation of Refractive Index for undoped and doped TiO_2

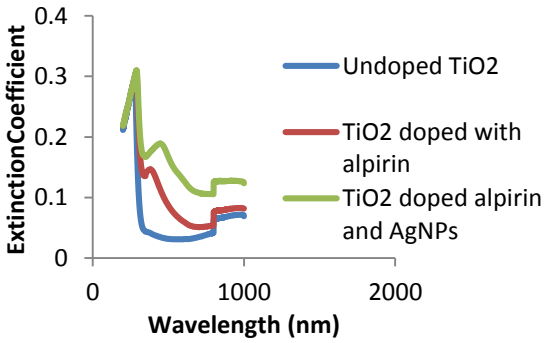

Fig. 5: Variation of Extinction Coefficient with wavelength for undoped and dope TiO_2

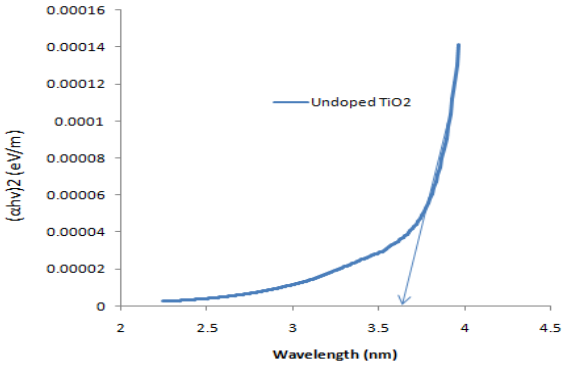

Fig. 6: Direct band gap for undoped TiO_2

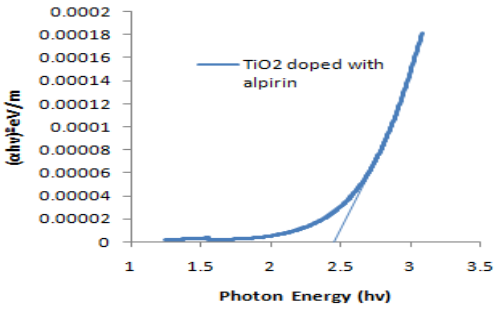

Fig. 7: A plot of $(\alpha h\nu)^2$ versus photon energy for TiO_2 doped with alpirin

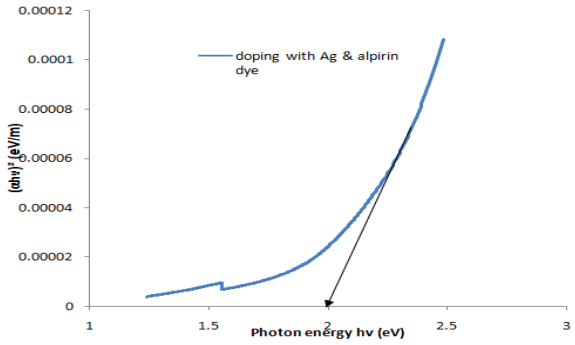

Fig. 8: A plot of $(\alpha h\nu)^2$ versus photon energy for TiO_2 doped with *alpirin*+ AgNPs

From Equation 7 the direct energy band gap of the films was evaluated at of zero y-axis of linear extrapolation of the plot. Figure 6 gives the direct band gap of 3.65 eV for undoped TiO_2, Figure 7 indicates 2.45 eV for *Alpirin*/TiO_2 and Figure 8 shows 2.00 eV for *Alpirin*/AgNPs/TiO_2. From these results, it is obvious that optical band gap energy of undoped TiO_2 decreased very well on doping with AgNPs + *alpirin* which allows delay in recombination of ion and increases photoactivities of TiO_2.

3.2: The X-ray Diffraction

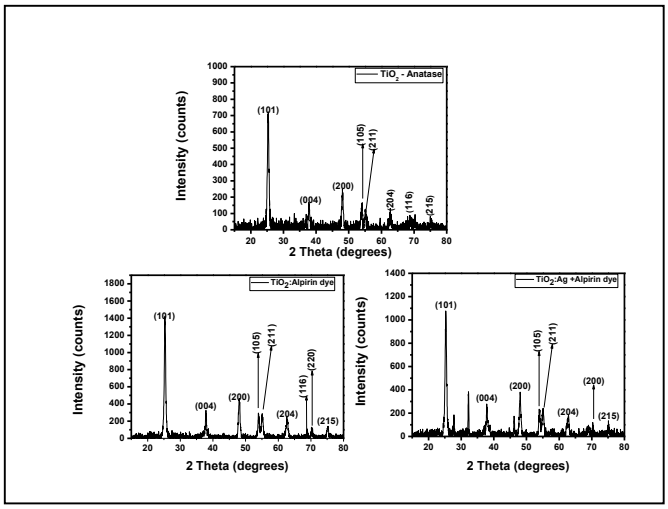

Fig. 9: XRD pattern for (a) undoped TiO_2 (b) TiO_2 doped with *Alpirin* (c) Ag and *alpirin* dye doped TiO_2 nanoparticles

The XRD pattern for the undoped TiO_2 with peaks at 2θ =25°, 38°, 48°, 54°, 55°, 63° and 75° which correspond to miller indices [101], [004], [200], [105], [211], [204], [116], and [215] as shown in Fig. 9(a). The patterns of deposited sample are attributed to reflections of anatase phase with tetragonal crystal structure. The results correspond to those obtained by Arishi et al., and Chenari et al., [5;22]. In Fig 9(b), there was phase transformation from amorphous to anatase and to rutile. It was also observed that the anatase phase with the tetragonal crystal structure has more peaks than the rutile phase. It is considered widely that this is as a result of improved charged carrier separation, possibly through the trapping of electrons in rutile and the consequent reduction in electron-hole recombination.

This result corresponds to those obtained by [30]. There are three additional peaks at 27.78°, 32.23° and 46.23° as shown in Fig. 9(c). The x–ray diffraction patterns is also attributed to reflections of anatase phase with tetragonal crystal structure, there is also the presence of Silver chlorargyrite AgCl. From Equation 5, the average crystallite sizes were 20.37 nm for undoped TiO_2, 21.39 nm for TiO_2 doped with *alpirin* and 18.26 nm for TiO_2 doped with Ag + *alpirin*. The average dislocation densities were calculated using Equation 9 by [31].

$$\delta = \frac{1}{D^2} \qquad (9)$$

The average dislocation densities were; $3.086 \times 10^{-3} lines/nm^2$ for undoped TiO_2, $2.597 \times 10^{-3} lines/nm^2$ for TiO_2 doped with *alpirin* and $3.093 \times 10^{-3}\ lines/nm^2$ for TiO_2 doped with Ag + *alpirin*. The XRD of the synthesized nanoparticles are very broad which indicates large crystallite sizes. Anatase TiO_2 is seen as the main polymorph present in the samples. The diffraction angles indicate a body centered tetragonal

crystalline structure of TiO_2. The peaks of the doped samples were shifted to the higher diffraction angles as compared to that of the undoped TiO_2 sample. The results show that average crystallite size of TiO_2 slightly increases when it was doped with *alpirin* and decreases when it was doped with Ag + *alpirin*.

3.3: EDS Spectra

In Figure 10, EDS spectra for *Alpirin*/AgNPs/TiO_2 sample revealed the presence of Titanium (Ti), and oxygen (O_2). Other element like silver (Ag), tin (Sn), chlorine (Cl) were also present due to deposition of Ag through SILAR cycle. The presence of phosphorus (P) and carbon (C) could be from the *alpirin* dye.

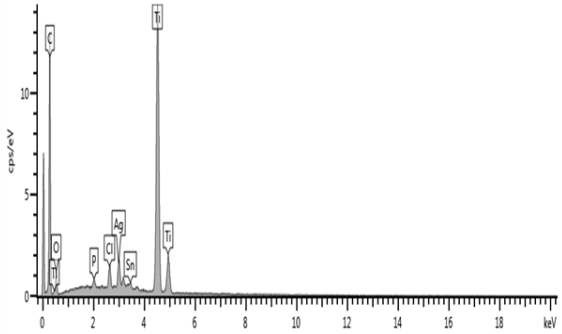

Fig.10: EDS image for TiO_2 doped with Ag and *alpirin* dye

Conclusion

In this research, the impact of *alpirin* and AgNPs + alpirin on the optical and structural properties of TiO_2 nanoparticles, synthesized using the screen-printing technology was investigated. The X-ray diffraction pattern showed crystalline nature of TiO_2. The results show enhanced absorption in the visible spectrum for both configurations but was more obvious in the combination of AgNPs + *alpirin.* The transmittance for the TiO_2 samples was high which lends good application as optical window solar cells. The refractive index increases for TiO_2 soaked in *alpirin* and increased further when soaked in Ag + *alpirin*. The average dislocation densities increase with decreasing particle size. Chemical composition of the sample was confirmed by EDS. Results obtained show high permeability as required in optical windows.

References

[1] A. Mbonyiryivuze, Z. Sidiki, D. Abdoulaye, B. Sone, M. Evariste, Y. Lakhan-Lal, M. Bonex, M. D. Simon

and M. Malik, "Titanium Dioxide Nanoparticles Biosynthesis for Dye Sensitized Solar Cells application," Review. *Phy. and Mat. Chem/Sc and Edu Pub*, vol 3, pp. 12-17. 2015.

[2] J. Nowotny, M. Radecka, M. Rekas, S. Sugihara, E. R. Vance, and W. Weppner, "Electronic and ionic conductivity of TiO_2 single crystal within the n-p transition range," *Int. J. of Cer*, vol. 24 page 571-577 1998.

[3] J. O. Ozuomba, and A. J. Ekpunobi, "A study of the band gap of sensitized Titanium dioxide nanoparticles and their photovoltaic applications," *Mold J. of the Phys. Sci.*, vol. 12 no 3-4, pp. 165-171, 2013.

[4] M. Kralova, D. Petr, V. Michal, and C. Jaroslav, " Preparation and characterization of doped titanium dioxide printed layers," *Cat. Tod., Els.*, vol. 230, pp. 188-196, 2014.

[5] J. I. Arishi, O. F. Nwosu, and O. Onumah, "Influence of Ag-doping on optical and structural properties of TiO_2 thin films deposited dye Electrohydrodynamic Spray Pyrolysis," *J. of Mat. Sci. Res. and Rev.*, vol. 2 no 3, pp 1-10, 2019.

[6] R. A. Donald, "The Science and Engineering of Materials," Ed vol. New York: Wadsworth, Inc. 1985.

[7] J. O. Ozuomba, A. J. Ekpunobi, and P. I. Ekwo, "The viability of a natural dye extracted from paw-paw leaves as photosensitizer for sensitized solar cell," *Intern. Sci. Res. J.*, vol. 3, pp. 3-5, 2011.

[8] J. X. Liu, D. Z. Yang, F. Shi, and Y. J. Cai, "Sol–gel deposited TiO film on NiTi surgical alloy for biocompatibility improvement," Thin Sol. Films, vol. 429, pp. 225-230, 2013.

[9] S. Janitabar-Darzi, A. R. Mahjoub, A. Bayat, "Synthesis and characterization of visiblelight active S-doped TiO_2 nanophotocatalyst," *Intern. J. of Nano Dim.*, vol. 7 pp. 33-40, 2016.

[10] P. Mehdizadeh, Z. Tavangar, N. Shabani, and M. Hamadanian, "Visible light activity of nitrogen-doped TiO_2 by Sol-gel method using various nitrogen sources," *J. of Nanost,* vol.10, no. 2, pp. 307-316, 2020.

[11] M. Monsefi, T. Tajerian, and A. Rowan, "Size-Controlled Synthesis of Gold Nanostars and Their Characterizations and Plasmon Resonances. *J Nanostruct*, 10(2), 198-205 2020.

[12] D. B. Alwan, F. H. Wesam, H. Ali, and A. A. Twej, "Improving the efficiency of dye-sensitized solar cells with doping and co-doping titanium dioxide," I*raqi Journal of Sci*, vol. 57(3C), pp. 2228-2233, 2016.

[13] U. R. Anees, A. Farooq, and K. A. Haseeb, "Analyze the absorption properties and I-V characterization of dye sensitized solar cell using ruthenium dye," Pak. Amer. *J. of Eng. and Appl. Sci.*, vol. 37, no. 8, pp. 611- 621, 2014.

[14] L. Su Pei, P. Alagarsamy, L. Hong-Ngee, R. Ramasamy, and H. Nay-Ming, "Boosting photovoltaic

performance of dye-sensitized solar cells using silver nanoparticle-decorated N,S-co-doped-TiO_2 photoanode," Sci. Rep., vol. 5, pp. 1-14, 2015.

[15] E. Danladi, J. Ezeoke, M. S. Ahmad, E. Danladi, S. H. Sarki, G. P. M. IshayaIliyasu, "Photoelectrochemical performance of dye-sensitized organic photovoltaic cells based on natural pigments and wide-bandgap nanostructured semiconductor," *Phy. Sci. Intern. J.*, vol. 10, no. 2, pp. 1-7, 2016.

[16] G. Govindasamy, P. Murugasen, and S. Sagadevan, "Investigations on the synthesis, optical and electrical properties of TiO_2 thin films by chemical bath deposition (CBD) method," *Mat. Res.*, vol.19, pp. 413-419, 2016.

[17] C. Huaimin, L. B. Da-Chen, and S. Kangying, "Hydrothermal synthesis and electrochemical properties of TiO_2 nanotubes as an anode material for lithium ion batteries. *Int. J. Electrochem. Sci.*, vol. 13, pp. 2118–2125, 2018 .

[18] S. A. Aliev, N. E. Nikolaev, N. S. Trofimov, and T. K. Chekhlova, "Properties of TiO_2 films with gold nanoparticles," Conference Series. Russia, International Conference of Photonics and Information Optics IOP Publishing *Journal of Physics*, vol.737, pp.1-8, 2016.

[19] M. Yu, S. V. Evtushenko, N. S. Romashkin, K. Trofimov, and T. K. Chekhlova, "Optical properties TiO_2 thin films," Elsev. Sci. Dir. pp. 100-107, 2015.

[20] B. A. Bregadiolli, S.L. Fernandesa, C. Graeff, and F. de Oliveira, "Easy and fast preparation of TiO_2 - based nanostructures using microwave assisted hydrothermal synthesis," *Mat. Res*., vol. 20, no. 4, pp. 912-919, 2017.

[21] J. M. Valtierra, S. C. Manuel, F. R. Claudio, and C. Sergio, "Formation of smooth and rough TiO_2 thin films on fibreglass by sol-gel method," *J. Mex. Chem. Soc*., vol. 50, no. 1, pp. 8-13, 2006.

[22] H. M. Chenari, S. Christoph, H. Dirk, R. Friedrich, and A. Hossein, "Titanium dioxide nanoparticles: synthesis, X-Ray line analysis and chemical composition," *Mat. Res. Stud*., vol.1, pp. 1-5, 2016.

[23] I. I. Dike, and M. N. Chukwu, "Visible light activity of enhaced screen-printed Titanium dioxide," *Act. Scient. Appl. Phy.* vol. 2, no. 9, pp. 22-27, 2022.

[24] V. Vetrivel, K. Rajendran, and V. Kalaiselvi, "Synthesis and characterization of pure titanium dioxide nanoparticles by Sol-gel method," *Intern. J. of Chem. Tech. Res*., vol. 7, no. 3, pp. 1090-1097, 2015.

[25] J. C. Johnson, "Inkjet printing of titanium dioxide photoanodes for dye sensitized solar cells," Grand Valley State, GVSU ScholarWork, 2013 accessed online on 27th August 2019,

[26] C. W. Foster, C. E. Banks, and R.O. Kadara, "Screen-printing electrochemical architectures," *Sprin.*

Bri. in Appl. Sci. and Techn., vol. 3, pp. 13-23, 2016.

[27] J. E. Khalil, "Natural dye-sensitized solar cell based on nanocrystalline TiO_2," *Sain. Malay.*, vol. 41, no. 8, pp. 1011–1016, 2012.

[28] U. I. Kasim, A. Umar, I. Adamu, I. K. Mohammed, U. E. Uno Essang, M. N. Muhammed and A. Noble, Springer, 3, 2-6, 2014.

[29] Barness and Alexander, "Impact of extraction methods upon light absorbance of natural organic dyes for dye sensitized solar cells application," J. of Ener. and Nat. Res., vol. 3, pp. 38-45, 2014. doi: 10.11648/j.jenr.20140303.13

[30] M. H. Shine, S. A. A. Al Saati, and F. Z. Razooqi, "Preparation of high transmittance TiO_2 thin films by sol-gel technique as antireflection coating*." J. of Phys: Conf. Series*, vol. 1032, no. 012018, pp. 1-12, 2018.

[31] I. I. Dike, and O. O. Ozuomba, Effect Of 0.1m Silver nanoparticleson the optical and structural properties of TiO_2 doped with *Alpirin* dye," ASPJ for SSE, vol. 1, no. 1, pp. 219-234, 2020.

[32] F. M. Tezel, O. Ozdemir, and I. A. Kariper, "The effects of pH on structural and optical characterization of Iron oxide thin films," *Surf. Rev. and Lett*., vol. 24, no. 4, pp. 1 – 10, 2017.

[33] A. Dorian, H. Hanaor, and C. S. Charles,"Review of the anatase to rutile phase transformation," *Sprin. J. of Mat. Sc*i., vol. 46, no. 4, pp. 855-874, 2017.

[34] F. Hajyakbary, J. Sietsma, A. J. Bottger, and M. J. Santofimia, **"**An improved X-ray diffraction analysis method to characterize dislocation density in lath martensitic structures," *Mat. Sci. and Eng.; Elsev*. Vol. 639, 2015.